

# Curvature Filtrations for Graph Generative Model Evaluation

Joshua Southern<sup>\*1</sup> Jeremy Wayland<sup>\*2,3</sup> Michael Bronstein<sup>4</sup> Bastian Rieck<sup>2,3</sup>

## Abstract

Graph generative model evaluation necessitates understanding differences between graphs on the distributional level. This entails being able to harness salient attributes of graphs in an efficient manner. Curvature constitutes one such property of graphs, and has recently started to prove useful in characterising graphs. Its expressive properties, stability, and practical utility in model evaluation remain largely unexplored, however. We combine graph curvature descriptors with cutting-edge methods from topological data analysis to obtain robust, expressive descriptors for evaluating graph generative models.

## 1. Introduction

Graph-structured data are prevalent in a number of different domains, including social networks (Monti et al., 2019), bioinformatics (Jumper et al., 2021; Ruiz et al., 2021), and transportation (Jiang & Luo, 2022). The ability to generate new graphs from a distribution is a burgeoning technology with promising applications in molecule or protein design Jin et al. (2018; 2021), as well as circuit design (Mirhoseini et al., 2021). To compare graph generative models and advance research in this area, it is essential to have a metric that can measure the distance between a set of generated and reference graphs. Typically, this is done by using a set of descriptor functions, which map a graph to a high-dimensional representation in  $\mathbb{R}^d$ . An evaluator function, such as the maximum mean discrepancy (Gretton et al., 2012, MMD), may then be used to get a distance between two distributions of graphs by comparing their vectorial representations (Liao et al., 2019; Niu et al., 2020). This state of the art was recently critiqued by O’Bray et al. (2022) since it (i) requires numerous parameter and function choices, (ii) is limited by the *expressivity* of the descriptor function, and (iii) does not come equipped with *stability guarantees*.

MMD is a powerful method to compare different distributions and can be directly combined with standard graph

kernels (Borgwardt et al., 2020) for graph distribution comparison. While there are several approaches for defining graph kernels, the most common one makes use of the  $\mathcal{R}$ -Convolution framework Haussler (1999), which defines the similarity between two graphs based on the similarity of their substructures. However, there are some subtle issues when calculating kernels in  $\mathbb{R}^d$ , e.g. Gaussian kernels on geodesic metric spaces have limited applicability when spaces have nonzero curvature (Feragen et al., 2015) and certain kernels in the literature are indefinite, thus violating one of the tenets of MMD.

We propose to overcome these issues through topological data analysis (TDA), which is capable of capturing multi-scale features of graphs, going well beyond simple descriptor functions. TDA is built on the existence of a function of the form  $f: V \rightarrow \mathbb{R}$ , or  $g: E \rightarrow \mathbb{R}$  on a graph  $G = (V, E)$ . This is used to obtain a *filtration*, i.e. an ordering of subgraphs, resulting in a set of topological descriptors, the *persistence diagrams*. Motivated by their expressive power and computational efficiency, we use recent notions of discrete curvature (Devriendt & Lambiotte, 2022; Forman, 2003; Ollivier, 2007) to define filtrations and calculate *persistence landscapes* (Bubenik, 2015) from the persistence diagrams, thus obtaining a descriptor whose Banach space formulation permits statistical calculations. Our proposed method comes equipped with stability guarantees, can count certain substructures and measure other important graph characteristics, and can be used to evaluate a variety of statistical tests since it provides the infrastructure for computing distances between graph distributions.

Our *contributions* are as follows:

- We provide a thorough theoretical analysis of the stability and expressivity of recent notions of discrete curvature, showing their fundamental utility for graph learning applications.
- We combine discrete curvature with TDA to obtain a novel metric for graph generative model evaluation.
- Our experiments reveal our metric is robust and expressive, thus improving upon current approaches based on simple graph descriptor and evaluator functions.

## 2. Background

The topological descriptors used in this paper are based on a combination of ideas from *computational topology* and

<sup>1</sup>Imperial College London <sup>2</sup>Helmholtz Munich <sup>3</sup>Technical University of Munich <sup>4</sup>University of Oxford. Correspondence to: Bastian Rieck <bastian.rieck@helmholtz-munich.de>.

*discrete curvature*. We give an overview of these areas and briefly comment on previous work that makes use of *graph statistics* in combination with *maximum mean discrepancy* (MMD). In the following, we consider undirected graphs, denoted  $G = (V, E)$ , with a set of vertices  $V$  and a set of edges  $E \subseteq V \times V$ .

## 2.1. Metrics Based On Graph Statistics

Graph generative models are conventionally evaluated using graph statistics (Dai et al., 2020; You et al., 2018). These approaches extract a feature vector from each graph, such as the clustering coefficient or node degree, which is then used to compute the empirical MMD between generated and reference sets. Some works (Moreno et al., 2018) have combined multiple structural properties of graphs into a single metric through the Kolmogorov–Smirnov (KS) multi-dimensional distance (Justel et al., 1997). Combining graph statistics into a single measure has also led to metrics between molecular graphs, such as the quantitative estimate of drug-likeness (QED), which is a common measure in drug discovery (Bickerton et al., 2012). However, these simple statistics, even when considered jointly, often lack expressivity, have no stability guarantees, and their use with MMD requires numerous parameter and function choices (O’Bray et al., 2022).

## 2.2. Computational Topology

Computational topology assigns *invariants*—characteristic properties that remain unchanged under certain transformations—to topological spaces. For graphs, the simplest invariants are given by the 0-dimensional ( $\beta_0$ ) and 1-dimensional ( $\beta_1$ ) Betti numbers. These correspond to the number of connected components and number of cycles, respectively, and can be computed efficiently. Their limited expressivity can be substantially increased when paired with a scalar-valued function  $f: V \rightarrow \mathbb{R}$ . Since  $f$  can only attain a finite number of values  $a_1, a_2, \dots$  on the graph, this permits calculating a *graph filtration*

$$\emptyset \subseteq G_0 \subseteq G_1 \dots \subseteq G_{k-1} \subseteq G_k = G, \quad (1)$$

where each  $G_i := (V_i, E_i)$ , with  $V_i := \{v \in V \mid f(v) \leq a_i\}$  and  $E_i := \{e \in E \mid \max_{v \in e} f(v) \leq a_i\}$ . This *sublevel set filtration* (swapping ‘ $\leq$ ’ for ‘ $\geq$ ’ and max for min results in the *superlevel set filtration*) permits tracking topological features, such as cycles, via *persistent homology*. If a topological feature appears for the first time in  $G_i$  and disappears in  $G_j$ , we can represent the feature as a tuple  $(a_i, a_j)$ , which we can collect in a *persistence diagram*  $D$ . Persistent homology thus tracks changes in connected components and cycles over the complete filtration, measured using a filtration function  $f$ . Persistence diagrams form a metric space, with the distance between them given by the

*bottleneck distance*, defined as

$$d_B(D, D') := \left( \inf_{\eta: D \rightarrow D'} \sup_{x \in D} \|x - \eta(x)\|_\infty \right), \quad (2)$$

where  $\eta$  ranges over all bijections between the two diagrams. A seminal *stability theorem* by Cohen-Steiner et al. (2007) states that the bottleneck distance between persistence diagrams  $D_f, D_g$ , generated from two functions  $f$  and  $g$  on the same graph, is upper-bounded by  $d_B(D_f, D_g) \leq \|f - g\|_\infty$ . The infinity norm of the functions, a geometrical quantity, hence limits the topological variation.

Persistent homology is appealing because of its expressivity and stability properties. The specific choice of filtration  $f$  is known to crucially affect expressivity: with a specific choice of filtration, persistent homology can be *more* expressive than the 1-WL test (Horn et al., 2022), which is commonly used to bound the expressivity of graph neural networks (Morris et al., 2019; Xu et al., 2019). Thus, given a suitable filtration, we can create a robust and expressive metric for comparing graphs. Moreover, as we will later see, TDA improves the expressivity of *any* filtration function, meaning that even if the function on its own is not capable of distinguishing between different graphs, using it in a filtration context can overcome these deficiencies.

## 2.3. Discrete Curvature

While filtrations can be learnt Hofer et al. (2020), in the absence of a well-defined learning task for graph generative model evaluation, we opt instead to employ existing functions that exhibit suitable expressivity properties. Of particular interest are functions based on *discrete curvature*, which was shown to be an expressive feature for graph learning tasks (Velingker et al., 2022). Curvature is a fundamental concept in differential geometry and topology, making it possible to distinguish between different types of manifolds. There are a variety of different curvature formulations with varying properties, with *Ricci curvature* being one of the most prominent. Roughly speaking, Ricci curvature is based on measuring the differences in the growth of volumes in a space as compared to a ‘model’ Euclidean space. While originally requiring a smooth setting, recent work started exploring how to formulate a theory of Ricci curvature in the discrete setting (Devriendt & Lambiotte, 2022; Forman, 2003; Liu et al., 2018; Ollivier, 2007; Saucan et al., 2020). Intuitively, discrete curvature measures quantify a notion of similarity between node neighbourhoods, the discrete concept corresponding to ‘volume’. They tend to be *larger* for structures where there are overlapping neighbourhoods such as cliques, *smaller* (or zero) for grids and *lowest* (or negative) for tree-like structures. Ricci curvature for graphs provides us with sophisticated tools to analyse the neighbourhood of an edge and recent works have shown the benefits of using some of these curvature-based methods in

combination with Graph Neural Networks (GNNs) to boost performance (Vellingker et al., 2022), assess differences between real-world networks (Samal et al., 2018), or enable *graph rewiring* to reduce over-squashing in GNNs (Topping et al., 2021). However, the representational power and stability properties of these measures remain largely unexplored. Subsequently, we will focus on three different types of curvature, (i) Forman–Ricci curvature (Forman, 2003), (ii) Ollivier–Ricci curvature (Ollivier, 2007), and (iii) Resistance curvature Devriendt & Lambiotte (2022). We find these three notions to be prototypical of discrete curvature measures, increasing in complexity and in their ability to capture *global* properties of a graph.

**Forman–Ricci Curvature.** The *Forman(–Ricci) curvature* for an edge  $(i, j) \in E$  is defined as

$$\kappa_{\text{FR}}(i, j) := 4 - d_i - d_j + 3|\#\Delta|, \quad (3)$$

where  $d_i$  is the degree of node  $i$  and  $|\#\Delta|$  is the number of 3-cycles (i.e. triangles) containing the adjacent nodes.

**Ollivier–Ricci Curvature.** Ollivier introduced a notion of curvature for metric spaces that measures the Wasserstein distance between Markov chains, i.e. random walks, defined on two nodes (Ollivier, 2007). Let  $G$  be a graph with some metric  $d_G$ , and  $\mu_v$  be a probability measure on  $G$  for node  $v \in V$ . The *Ollivier–Ricci curvature* of an edge  $(i, j) \in E$  is then defined as

$$\kappa_{\text{OR}}(i, j) := 1 - \frac{1}{d_G(i, j)} W_1(\mu_i, \mu_j), \quad (4)$$

where  $W_1$  refers to the first *Wasserstein distance* between  $\mu_i, \mu_j$ . Eq. (4) defines the Ollivier–Ricci (OR) curvature in a general setting outlined by van der Hoorn et al. (2020); this is in contrast to the majority of previous works in the graph setting which specify  $d_G$  to be the shortest-path distance and  $\mu_i, \mu_j$  to be uniform probability measures in the 1-hop neighbourhood of the node. Extending the probability measures so that they act on larger locality scales is known to be beneficial for characterising graphs (Benjamin et al., 2021; Gosztolai & Arnaudon, 2021; Jiradilok & Kamtue, 2021). We assume this general setting to define different notions of OR curvature on the graph, permitting us the flexibility of altering the probability measure and the metric.

**Resistance Curvature.** The resistance curvature for edges of a graph, as established in Devriendt & Lambiotte (2022), is inspired by Ohm’s Law and the concept of effective resistance, a well-studied, global metric between nodes in a weighted graph that quantifies the resistance exerted by the network when current flows between nodes. For a graph  $G = (V, E, w)$ , let  $R_{ij}$  be the resistance distance between nodes  $i, j \in V$ , defined in Eq. (17), and  $w_{ij}$  the weight

between them if  $i \sim j$ . The *node resistance curvature* of a node  $i \in V$  is then defined as

$$p_i := 1 - \frac{1}{2} \sum_{j \sim i} R_{ji} w_{ji}. \quad (5)$$

The curvature of an edge  $(i, j) \in E$ , what we refer to as *resistance curvature*, is then defined as

$$\kappa_{\text{R}}(i, j) := \frac{2(p_i + p_j)}{R_{ij}} \quad (6)$$

The resistance curvature of an edge is related to the average distance between the neighbourhoods of the nodes connected by the edge.

### 3. Our Method

We use different notions of discrete curvature to define a set of graph filtrations. In combination with persistent homology, this enables us to assess the structural properties of a given graph at multiple scales. Using metrics on aggregated topological signatures—here, in the form of *persistence landscapes*—we may then compare two distributions of graphs. Specifically, we propose the following scheme for graph generative model evaluation:

1. Given a specific curvature filtration, we generate a set of *persistence diagrams* from the graph, encoding the persistent homology in dimensions 0 and 1 for each graph in the distribution. Each diagram encodes the lifespan of connected components and cycles as they appear in the filtration, resulting in a multi-scale summary of the graph’s structure.
2. To permit an analysis on the distributional level, we convert each diagram into a more suitable representation, namely a *persistence landscape*.
3. As functional summaries of topological information, persistence landscapes allow for easy calculation of averages and distances (Bubenik, 2015). Therefore, we conduct statistical comparisons between graph distributions, e.g. permutation tests, using  $p$ -norms in this latent space.

Figure 1 illustrates our proposed pipeline using Forman–Ricci curvature.

#### 3.1. Stability

We first discuss the general stability of our topology-based formulation, proving that changes in topological dissimilarity are bounded by changes in the respective filtration functions. Following this, we show that filtrations based on discrete curvature satisfy such stability properties if the underlying graph is modified.

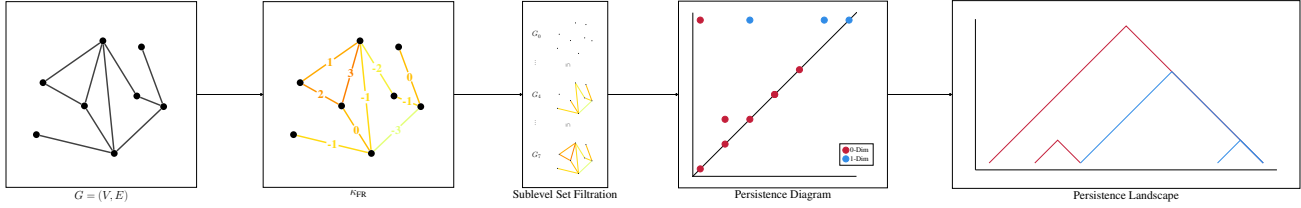


Figure 1: An overview of our pipeline for evaluating graph generative models using discrete curvature. We depict a graph’s edges being coloured by  $\kappa_{FR}$ , as described in Eq. (3). The ordering on edges gives rise to a *sublevel set filtration*, followed by a corresponding persistence diagram and landscape. For graph generative models, we select a curvature, apply this framework element-wise, and evaluate the similarity of the generated and reference distributions by comparing their average landscapes.

### 3.1.1. STABILITY OF TOPOLOGICAL FEATURES

As a consequence of the persistent homology stability theorem, we know that if two notions of curvature are similar on a graph, their corresponding persistence diagrams are also similar. However, the theorem only holds for two different functions on the *same* graph, whereas the distributional case has not yet been addressed by the literature. First, we show that our setting affords an upper bound.

**Theorem 1.** *Given two graphs  $F = (V_F, E_F)$  and  $G = (V_G, E_G)$  with scalar-valued filtration functions  $f, g$ , and their respective persistence diagrams  $D_f, D_g$ , we have*

$$d_B(D_f, D_g) \leq \max\{\text{dis}(f, g), \text{dis}(g, f)\}, \quad (7)$$

where  $\text{dis}(f, g) := |\max_{x \in V_F} f(x) - \min_{y \in V_G} g(y)|$  and vice versa for  $\text{dis}(g, f)$ .

The implication of this upper bound, which is not as tight as the stability theorem on the same graph, is that changes on the level of persistence diagrams are bounded by changes between the input functions. As we will prove later, all curvature notions satisfy stability properties of this form under graph perturbations, meaning that our method also remains bounded.

### 3.1.2. STABILITY OF DISCRETE CURVATURE

Having seen that the stability of our method hinges on the properties of the filtration functions, we now analyse the behaviour of the curvature functions themselves under perturbation. Following previous work (O’Bray et al., 2022), we aim to understand and quantify the stability of our method in response to adding and deleting edges in the graph. Our stability theorems establish bounds on various discrete curvature measures for *finite, unweighted, connected* graphs in response to these perturbations. Moreover, we restrict the outcome of a perturbation to graphs of the form  $G' = (V, E')$  that satisfy  $|E| \neq |E'|$  and do not change the number of connected components of a graph. Our theoretical results bound the new curvature  $\kappa'$  according to the structural properties  $G$ . For an exhaustive list of theorems and proofs, as

well as experiments analysing the change in curvature for perturbed Erdős–Rényi (ER) graphs, see Appendix C and Appendix A.

**Forman–Ricci Curvature.** Let  $G$  be an unweighted, connected graph with Forman curvature  $\kappa_{FR}$  defined over the edges in  $E$ .

**Theorem 2.** *If  $G'$  is the graph generated by **edge addition**, then the updated Forman curvature  $\kappa'_{FR}$  for pre-existing edges  $(i, j) \in E$  can be bounded by:*

$$\kappa_{FR}(i, j) - 1 \leq \kappa'_{FR}(i, j) \leq \kappa_{FR}(i, j) + 2. \quad (8)$$

**Theorem 3.** *If  $G'$  is the graph generated by **edge deletion**, then the updated Forman curvature  $\kappa'_{FR}$  for pre-existing edges  $(i, j) \in E$  can be bounded as follows:*

$$\kappa_{FR}(i, j) - 2 \leq \kappa'_{FR}(i, j) \leq \kappa_{FR}(i, j) + 1. \quad (9)$$

**Ollivier–Ricci Curvature.** Consider the following triple that specifies an OR curvature computation:  $\mathcal{G} = (G, d_G, \mu)$  where  $G$  is an unweighted, connected graph,  $d_G$  is the associated graph metric, and  $\mu := \{\mu_v : v \in V\}$  is the collection of probability measures at each node. Furthermore, let  $\delta_i$  denote the Dirac measure at node  $i$  and  $J(i) := W_1(\delta_i, \mu_i)$  the corresponding jump probability in the graph  $G$  as defined in Ollivier (2007). Following an edge addition or deletion, we consider an updated triple  $\mathcal{G}' = (G', d_{G'}, \mu')$ , and remark that this yields an updated Wasserstein distance  $W'_1$ , calculated in terms of the new graph metric  $d_{G'}$ .

**Theorem 4.** *Given a perturbation producing  $\mathcal{G}'$ ,  $\kappa'_{OR}$  can be bounded above using  $d_{G'}$  and jump probabilities  $J'(v) = W'_1(\delta_v, \mu'_v)$ :*

$$\kappa'_{OR} \leq \frac{J'(i) + J'(j)}{d_{G'}(i, j)}. \quad (10)$$

A lower bound for OR curvature in the event of edge addition *or* deletion can be specified in terms of the maximal reaction (as measured by the updated Wasserstein distance) to the perturbation,  $W'_{\max} := \max_{x \in V} W'_1(\mu_x, \mu'_x)$ .

**Theorem 5.** Given a perturbation that yields  $\mathcal{G}' = (G, d_{G'}, \mu')$ ,  $\kappa'_{OR}$  can be bounded below by:

$$\kappa'_{OR}(i, j) \geq 1 - \frac{1}{d_{G'}(i, j)} [2W'_{\max} + W'_1(\mu_i, \mu_j)]. \quad (11)$$

**Resistance Curvature.** Let  $G$  be an unweighted, connected graph with a resistance distance  $R_{ij}$  and resistance curvature  $\kappa_R(i, j)$  for each  $(i, j) \in E$ . Furthermore, let  $d_x$  denote the degree for node  $x \in V$  and  $N$  be the normalized Laplacian matrix of  $G$  as defined in Lovász (1996). We find that  $\kappa_R$  is well-behaved under these perturbations, in the sense that edge additions can only *increase* the curvature, and edge deletions can only *decrease* it, and provide the corresponding bounds.

**Theorem 6.** If  $G'$  is the graph generated by *edge addition*, then  $\kappa'_R \geq \kappa_R$ , with the following bound:

$$|\kappa'_R(i, j) - \kappa_R(i, j)| \leq \frac{\Delta_{add}(d_i + d_j)}{R_{ij} - \Delta_{add}}, \quad (12)$$

where  $\Delta_{add} := \max_{i, j \in V} (R_{ij} - \frac{1}{2}(\frac{1}{d_i+1} + \frac{1}{d_j+1}))$ .

**Theorem 7.** If  $G'$  is the graph generated by *edge deletion*, then  $\kappa'_R \leq \kappa_R$ , bounded by:

$$\frac{|\kappa'_R(i, j) - \kappa_R(i, j)|}{R_{ij} + \Delta_{del}} \leq \frac{2}{R_{ij}} [(2R_{ij} + \Delta_{del})(p_i + p_j) - \Delta_{del}(d_i + d_j)],$$

where  $\Delta_{del} = \frac{2}{1-\lambda_2} - \min_{i, j \in V} (R_{ij})$  and  $\lambda_2$  is the second largest eigenvalue of  $N$ .

**Summary.** The implications of this section are that (i) the stability of our topological calculations largely hinges on the stability of the functions being used to define said filtrations, and (ii) *all* discrete curvature measures satisfy stability properties with respect to changes in graph connectivity, making curvature-based filtrations highly robust.

### 3.2. Expressivity

A metric between distributions should be non-zero when the distributions differ. For this to occur, our metric needs to be able to distinguish non-isomorphic graphs and be sufficiently expressive. Horn et al. (2022) showed that persistent homology with an appropriate choice of filtration is strictly more expressive than 1-WL. A similar expressivity result can be obtained for using resistance curvature as a node feature (Velingker et al., 2022), underlining the general utility of curvature. We have the following general results concerning the expressivity or discriminative power of our topological representations.

**Theorem 8.** Given two graphs  $F = (V_F, E_F)$  and  $G = (V_G, E_G)$  with scalar-valued filtration functions  $f, g$ , and their respective persistence diagrams  $D_f, D_g$ , we have

$$d_B(D_f, D_g) \geq \inf_{\eta: V_F \rightarrow V_G} \sup_{x \in V_F} |f(x) - g(\eta(x))|, \quad (13)$$

where  $\eta$  ranges over all maps from  $V_F$  to  $V_G$ .

Theorem 8 implies that topological distances are more discriminative than distances between functions. Thus, calculating topological representations of graphs based on a class of functions improves discriminative power.

To further understand the expressive power of curvature filtrations, we analyse strongly-regular graphs, which are often used for studying GNN expressivity as they cannot be distinguished by 1-WL or 3-WL (Arvind et al., 2018; Bodnar et al., 2021). Additionally, we explore how curvature filtrations can count substructures, an important tool for evaluating and comparing expressivity (Papp & Watenhofer, 2022). To the best of our knowledge, ours is the first work to explore discrete curvature and curvature-based filtrations in this context.

#### 3.2.1. DISTINGUISHING STRONGLY REGULAR GRAPHS

Strongly regular graphs are often used to assess the expressive power of graph learning algorithms, constituting a class of graphs that are particularly hard to distinguish. Here, we assess the ability of curvature and curvature-based filtrations to discriminate between non-isomorphic graphs.

We briefly recall some definitions. A connected graph  $G$  with diameter  $D$  is called distance-regular if there are integers  $b_i, c_i$ , ( $0 \leq i \leq D$ ) such that for any two vertices  $x, y \in V$  with  $d(x, y) = i$ , there are  $c_i$  neighbours of  $y$  in  $k_{i-1}(x)$  and  $b_i$  neighbours of  $y$  in  $k_{i+1}(x)$ . For a distance-regular graph, the intersection array is given by  $\{b_0, b_1, \dots, b_{D-1}; c_1, c_2, \dots, c_D\}$ . A graph is called *strongly-regular* if it is distance-regular and has a diameter of 2 (Dam et al., 2016). We first state three theoretical results about curvature.

**Proposition 1.** Both Forman–Ricci curvature and Resistance curvature cannot distinguish distance-regular graphs with the same intersection array.

**Proposition 2.** Ollivier–Ricci curvature can distinguish the Rook and Shrikhande graphs, which are strongly-regular graphs with the same intersection array.

Notice that the Rook and Shrikhande graphs cannot be distinguished by 2-WL (Bouritsas et al., 2022) but OR curvature is sensitive to differences in their first hop peripheral subgraphs (Feng et al., 2022) and is able to distinguish them. These propositions show the limitations of Forman and resistance curvature as well as the potential benefit of using

OR curvature. We further evaluated the curvature measures and their filtrations on strongly-regular graphs in the experimental section, showing improvements in distinguishability by incorporating TDA.

### 3.2.2. COUNTING SUBSTRUCTURES

Evaluating the ability of curvature to encode structural information is a crucial aspect for understanding its expressivity and validating its overall utility in graph learning. It has previously been shown that incorporating structural information of graphs can extend the expressive power of message-passing neural networks (Chen et al., 2019; Geerts et al., 2020; Li et al., 2019). Additionally, Bouritsas et al. (2022) show how GNNs can be (i) strictly more expressive than 1-WL by counting local isomorphic substructures (e.g. cliques), and (ii) exhibit predictive performance improvements when adding such substructure counts to the node features. For instance, some strongly-regular graphs can be distinguished by counting 4-cliques. Discrete curvature measures are informed by these local substructures and have been shown to improve expressivity beyond 1-WL (Velingker et al., 2022) when included as a node feature. Nevertheless, there is limited work exploring what substructure information curvature carries, which would allow us to describe the expressivity of the measure.

The difference in perspective between the three prototypical curvatures discussed in this paper is underscored by their respective abilities and biases towards counting substructures: *Forman curvature* is an inherently local measure by definition, depending only on 3-cycles between adjacent nodes and their degrees. *Ollivier–Ricci curvature*, when used with a uniform measure, can bound the number of triangles within a locally finite graph (Jost & Liu, 2011) through its relation with the Watts–Strogatz clustering coefficient (Watts & Strogatz, 1998). It can also be shown that quadrangles and pentagons influence the OR curvature, further enhancing the expressivity of this type of curvature (Jost & Liu, 2011). This is the most global perspective one can achieve using  $\kappa_{\text{OR}}$  with uniform probability measures, since polygons with more than five edges do not impact the curvature valuation. However, by changing the probability measure used by  $\kappa_{\text{OR}}$ , we can shift the focus towards even larger substructures. For example, the  $n$ th power of the transition matrix provides information on the number of  $n$ -paths and can therefore provide substructure information for cycles of size  $n$  (Li et al., 2020). *Resistance curvature*, by contrast, is biased towards the largest substructures, complementing the flexibility of OR and the efficiency of Forman. Due to the ‘global’ nature of the resistance distance metric,  $\kappa_{\text{R}}$  assigns cycles of size  $\geq 5$  a positive curvature. Moreover, in a locally finite graph, one cannot use  $\kappa_{\text{R}}$  to establish a non-trivial bound on the number of triangles (consider creating an infinite cycle between two nodes).

*Table 1:* Success rate ( $\uparrow$ ) of distinguishing pairs of strongly-regular graphs when using either raw discrete curvature values, or a curvature filtration.

Data	$\kappa_{\text{FR}}$	$\kappa_{\text{OR}}$	$\kappa_{\text{R}}$	$\kappa_{\text{FR}}$	$\kappa_{\text{OR}}$	$\kappa_{\text{R}}$
	Raw			Filtration		
sr16622	0.00	1.00	0.00	1.00	1.00	1.00
sr261034	0.00	0.78	0.00	0.20	0.89	0.20
sr281264	0.00	1.00	0.00	0.00	1.00	0.00
sr361446	0.00	0.00	0.00	0.02	0.02	0.02
sr401224	0.00	0.00	0.00	0.93	0.93	0.93

Finally, we remark that persistent homology can also track the number of cycles over the filtration of interest, allowing further structural information to be encoded at multiple scales. Thus, we will subsequently experimentally explore the extent to which substructures can be counted for different curvatures (with and without a topological component), providing evidence on the expressive power of our approach.

## 4. Experiments

We have proven the theoretical stability of discrete curvature notions under certain graph perturbations. We also illustrated their ability to distinguish distance-regular and strongly-regular graphs. Subsequently, we will discuss empirical experiments to evaluate these claims and to further test the utility of our methods.

### 4.1. Distinguishing Strongly-Regular Graphs

In addition to the theoretical arguments outlined, we explored the ability of our method to distinguish strongly-regular graphs in a subset of data sets, i.e. sr16622, sr261034, sr281264, sr361446, and sr401224. These data sets are known to be challenging to classify since they cannot be described in terms of the 1-WL test (Bodnar et al., 2021). Our main goal is *not* to obtain the best accuracy, but to show how the discriminative power of discrete curvature can be improved by using it in a filtration context. Table 1 depicts the results of our classification experiment. We perform a pairwise analysis of all graphs in the data set, calculating distances based on histograms of discrete curvature measurements (‘raw’), or based on the bottleneck distance between persistence diagrams (‘TDA’). Subsequently, we count all non-zero distances ( $> 1 \times 10^{-8}$  to correct for precision errors).

Our main observation is that *combining TDA with curvature is always better than or equal to curvature without TDA*. Similar to the theoretical predictions, both resistance curvature and Forman curvature fail to distinguish any of the graphs without TDA. We therefore show the benefits from an expressivity point of view for using discrete curvature

Table 2: Pearson correlation ( $\uparrow$ ) of measures when adding/removing edges. Except for the filtrations, we use MMD to measure distances between distributions.

Measure	Adding Edges	Removing Edges
Laplacian	0.46	0.42
Clustering Coefficient	0.48	0.50
Degrees	0.76	1.00
$\kappa_{FR}$	0.42	0.43
$\kappa_{OR}$	0.90	0.91
$\kappa_R$	0.42	0.44
Filtration ( $\kappa_{FR}$ )	0.57	1.00
Filtration ( $\kappa_{OR}$ )	1.00	0.97
Filtration ( $\kappa_R$ )	0.73	0.95

as a filtration. Notably, we achieve the best results with OR curvature, which is particularly flexible since it permits changing the underlying *probability measure*. Using a probability measure based on random walks (see Appendix D) takes into account higher-order neighbourhoods and improves discriminative power (on `sr261034`, the pairwise success rate drops to 0.0/0.2 with raw/TDA values, respectively, if the uniform probability measure is used).

#### 4.2. Behaviour with Respect to Perturbations

To explore the behaviour of curvature descriptors under perturbations, we analyse the correlation of our metric when adding and removing edges in the Community Graph dataset. Specifically, we increase the fraction of edges added or removed from 0.0 to 0.95, measuring the distance between the perturbed graphs and the original graphs for each perturbation level. Following O’Bray et al. (2022), we require a suitable distance measure to be highly correlated with increasing amounts of perturbation. We compare to current approaches which use descriptor functions with MMD.

As Table 2 shows, a curvature filtration yields a higher correlation than curvature in combination with MMD, showing the benefits of employing TDA from a stability perspective. Additionally, curvature filtrations improve upon the normalized Laplacian and clustering coefficient. OR curvature exhibits particularly strong results when adding/removing edges, even surpassing the local degrees of a graph (which, while being well-aligned with perturbations of the graph structure, suffer in terms of overall expressivity).

#### 4.3. Counting Substructures

The ability of a descriptor to count local substructures is important for evaluating its expressive power (Barceló et al., 2021). We follow Chen et al. (2020), who assess the ability of GNNs to count substructures such as triangles, chordal cycles, stars and tailed triangles. This is achieved by generating regular graphs with random edges removed, and

Table 3: MAE ( $\downarrow$ ) for counting substructures based on raw curvature values and curvature-based filtrations. The Trivial Predictor always outputs the mean training target.

Method	Triangle	Tailed Tri.	Star	4-Cycle
Trivial Predictor	0.88	0.90	0.81	0.93
GCN	0.42	0.32	<b>0.1798</b>	<b>0.2822</b>
$\kappa_{FR}$	0.54	0.56	0.72	0.53
$\kappa_{OR}$	0.33	0.31	0.40	0.31
$\kappa_R$	0.59	0.50	0.72	0.47
Filtration ( $\kappa_{FR}$ )	0.45	0.52	0.49	0.60
Filtration ( $\kappa_{OR}$ )	<b>0.2321</b>	<b>0.2395</b>	0.34	0.31
Filtration ( $\kappa_R$ )	0.47	0.48	0.36	0.42

counting the number of occurrences of each substructure in a given graph. To assess the power of curvature to capture such local structural features, we pass the edge-based curvatures through a simple 1-layer MLP to output the substructure count. Additionally, we evaluate the effect of using the curvature as a filtration in the same manner.

Table 3 shows that OR curvature improves upon Graph Convolutional Networks (Kipf & Welling, 2016) in counting small local structures such as triangles and tailed triangles; this is a surprising finding given the smaller computational footprint of this curvature formulation (in comparison to a GCN). Moreover, we find that the OR curvature performs better than both the Forman curvature and the resistance curvature for the different substructures in the data. We also observe that combining curvature with TDA almost always improves upon using the curvature alone, the only exception being Forman curvature for counting 4-cycles.

#### 4.4. Synthetic Graph Generative Model Evaluation

To have a ground truth for a graph distribution, we tested our metric’s ability to *distinguish graphons*. Following the approach suggested by Sabanayagam et al. (2021), we generate four graphons,  $W_1(u, v) = uv$ ,  $W_2(u, v) = \exp\{-\max(u, v)^{0.75}\}$ ,  $W_3(u, v) = \exp\{-0.5 * (\min(u, v) + u^{0.5} + v^{0.5})\}$  and  $W_4(u, v) = \|u - v\|$ . Sampling from these graphons produces dense graphs, and we control their size to be between 9 and 37 nodes, thus ensuring that we match the sizes of molecular graphs in the ZINC dataset (Irwin & Shoichet, 2005), an important application for generative models.

We perform experiments by considering all combinations of three and four graphons, and we use distances between graphs, generated with a metric, in combination with spectral clustering to separate the distributions. We measure the performance of the algorithms using the Adjusted Rand Index (ARI) of the predicted clusters, comparing to two state of the art, kernel-based approaches: (i) Wasserstein Weisfeiler–Lehman graph kernels (Togninalli et al., 2019),

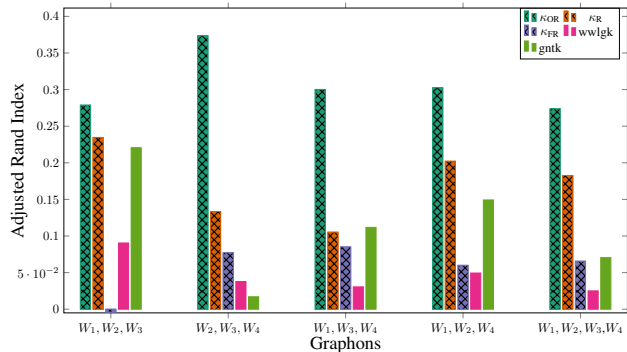


Figure 2: Adjusted Rand Index ( $\uparrow$ ) for clustering sets of four graphons. We compare our curvature filtrations ( $\boxtimes$ ) to kernel-based approaches.

and (ii) graph neural tangent kernels (Du et al., 2019). From Figure 2, we find that a filtration based on OR curvature is better able to distinguish and cluster graphons than the previously-described approaches based on kernels and it performs best for all sets of graphons.

We also notice that OR curvature performs better than other discrete curvatures, with resistance curvature achieving higher ARI than Forman curvature. Notice that unlike these kernel approaches, our method can be easily extended to provide a proper metric between distributions of graphs.

#### 4.5. Real-World Graph Generative Model Evaluation

By converting the generated persistence diagrams into a *persistence landscape*, we can generate an average topological descriptor for all graphs in a distribution (Bubenik, 2015). This allows us to calculate norms between graph distributions, making it possible to perform two-sample and permutation testing, unlike a majority of kernel-based approaches, which provide a distance between *all* individual graphs, or would require MMD to assess mean similarities. We randomly sample ten graphs from four different bioinformatics datasets, i.e. KKI, PROTEINS, Peking, and ENZYMES (Morris et al., 2020). We measure the distance between two datasets using the  $L^p$  norm between their average persistence landscapes. We then permute the two sets of graphs, measure the distance again, and generate the fraction of distances which are higher than the original. A low fraction indicates that distances are lower for permutations than between the original sets of graphs, suggesting that the metric can distinguish between the two distributions. We compare our approach to previous methods combining graph statistics with MMD.

If we set the permutation testing threshold to be  $p < 0.05$ , we see in Figure 3 that Forman and the OR curvature are able to distinguish *all but one pair of data sets*, an improvement over all the other approaches. In general, we find that

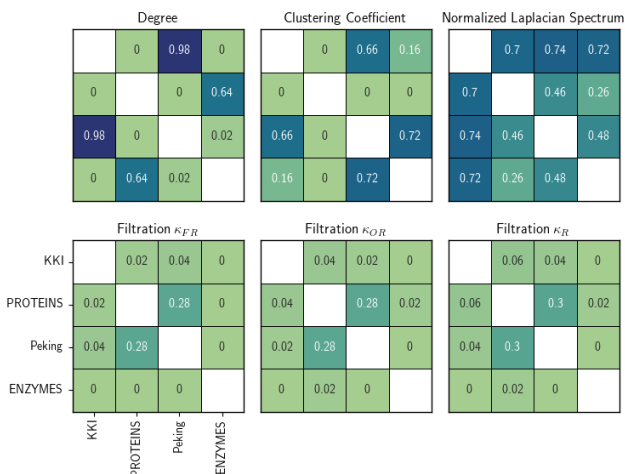


Figure 3: Permutation testing values ( $\downarrow$ ) for distinguishing different bioinformatics datasets. Position  $(i, j)$  in each matrix corresponds to a permutation test between dataset  $i$  and dataset  $j$ .

fractions are lower using curvature filtrations than graph statistic based approaches, demonstrating the utility of our approach.

## 5. Conclusion

We have described the first thorough analysis of the stability and expressivity of curvature and its filtration formulation on graphs. We believe this to be important for the community in multiple ways, from improving expressivity of GNNs to understanding curvature’s robustness on graphs. We propose using curvature filtrations and the persistence landscapes that they produce to measure distances between graph distributions. Our metric can be used for evaluating graph generative models, is robust and expressive, and improves upon current approaches based on descriptor and evaluator functions.

**Future work.** We have proposed a general framework for graph generative model evaluation, combining curvature with TDA. Future work could explore representations other than landscapes, new curvature measures, or extend our stability and expressivity results further. Another relevant direction involves incorporating node and edge features into the distance measure and applying the model to specific use cases such as evaluating molecule generation. We envisage that this could be done using bi-filtrations or by incorporating node features into the curvature itself.



## References

- Arvind, V., Fuhlbrück, F., Köbler, J., and Verbitsky, O. On weisfeiler-leman invariance: Subgraph counts and related graph properties, 2018. URL <https://arxiv.org/abs/1811.04801>.
- Barceló, P., Geerts, F., Reutter, J., and Ryschkov, M. Graph neural networks with local graph parameters, 2021. URL <https://arxiv.org/abs/2106.06707>.
- Benjamin, S., Mantri, A., and Perian, Q. On the wasserstein distance between  $k$ -step probability measures on finite graphs, 2021. URL <https://arxiv.org/abs/2110.10363>.
- Bickerton, G. R., Paolini, G. V., Besnard, J., Muresan, S., and Hopkins, A. L. Quantifying the chemical beauty of drugs. *Nat. Chem.*, 4(2):90–98, January 2012.
- Biggs, N. L. Potential theory on distance-regular graphs. *Combinatorics, Probability and Computing*, 2(3): 243–255, 1993. doi: 10.1017/S096354830000064X.
- Bodnar, C., Frasca, F., Wang, Y., Otter, N., Montufar, G. F., Lió, P., and Bronstein, M. Weisfeiler and Lehman go topological: Message passing simplicial networks. In Meila, M. and Zhang, T. (eds.), *Proceedings of the 38th International Conference on Machine Learning*, volume 139 of *Proceedings of Machine Learning Research*, pp. 1026–1037. PMLR, 2021.
- Borgwardt, K., Ghisu, E., Llinares-López, F., O’Bray, L., and Rieck, B. Graph kernels: State-of-the-art and future challenges. *Foundations and Trends® in Machine Learning*, 13(5–6):531–712, 2020. ISSN 1935-8237. doi: 10.1561/22000000076.
- Bouritsas, G., Frasca, F., Zafeiriou, S. P., and Bronstein, M. Improving graph neural network expressivity via subgraph isomorphism counting. *IEEE Transactions on Pattern Analysis and Machine Intelligence*, pp. 1–1, 2022. doi: 10.1109/TPAMI.2022.3154319.
- Bubenik, P. Statistical topological data analysis using persistence landscapes. *Journal of Machine Learning Research*, 16:77–102, January 2015.
- Chen, T., Bian, S., and Sun, Y. Are powerful graph neural nets necessary? A dissection on graph classification, 2019. URL <https://arxiv.org/abs/1905.04579>.
- Chen, Z., Chen, L., Villar, S., and Bruna, J. Can graph neural networks count substructures? 2020. doi: 10.48550/ARXIV.2002.04025. URL <https://arxiv.org/abs/2002.04025>.
- Cohen-Steiner, D., Edelsbrunner, H., and Harer, J. Stability of persistence diagrams. *Discrete & Computational Geometry*, 37(1):103–120, Jan 2007. doi: 10.1007/s00454-006-1276-5.
- Dai, H., Nazi, A., Li, Y., Dai, B., and Schuurmans, D. Scalable deep generative modeling for sparse graphs, 2020. URL <https://arxiv.org/abs/2006.15502>.
- Dam, E. R. V., Koolen, J. H., and Tanaka, H. Distance-regular graphs. *The Electronic Journal of Combinatorics*, 1000, apr 2016. doi: 10.37236/4925.
- Devriendt, K. and Lambiotte, R. Discrete curvature on graphs from the effective resistance, March 2022. URL <http://arxiv.org/abs/2201.06385>.
- Du, S. S., Hou, K., Póczos, B., Salakhutdinov, R., Wang, R., and Xu, K. Graph neural tangent kernel: Fusing graph neural networks with graph kernels, 2019. URL <https://arxiv.org/abs/1905.13192>.
- Feng, J., Chen, Y., Li, F., Sarkar, A., and Zhang, M. How powerful are  $k$ -hop message passing graph neural networks, 2022. URL <https://arxiv.org/abs/2205.13328>.
- Feragen, A., Lauze, F., and Hauberg, S. Geodesic exponential kernels: When curvature and linearity conflict. In *IEEE Conference on Computer Vision and Pattern Recognition (CVPR)*, pp. 3032–3042, 2015.
- Forman. Bochner’s method for cell complexes and combinatorial ricci curvature. *Discrete & Computational Geometry*, 29(3):323–374, Feb 2003. ISSN 1432-0444. doi: 10.1007/s00454-002-0743-x.
- Geerts, F., Mazowiecki, F., and Pérez, G. A. Let’s agree to degree: Comparing graph convolutional networks in the message-passing framework, 2020. URL <https://arxiv.org/abs/2004.02593>.
- Gosztolai, A. and Arnaudon, A. Unfolding the multiscale structure of networks with dynamical ollivier-ricci curvature. *Nature Communications*, 12(1):4561, Jul 2021. ISSN 2041-1723. doi: 10.1038/s41467-021-24884-1.
- Gretton, A., Borgwardt, K. M., Rasch, M. J., Schölkopf, B., and Smola, A. A kernel two-sample test. *Journal of Machine Learning Research*, 13(25):723–773, 2012.
- Guo, J.-M., Tong, P.-P., Li, J., Shiu, W. C., and Wang, Z.-W. The effect on eigenvalues of connected graphs by adding edges. *Linear Algebra and its Applications*, 548:57–65, July 2018. doi: 10.1016/j.laa.2018.02.012.
- Haussler, D. Convolution kernels on discrete structures ucsc crl. 1999.

- Hofer, C. D., Graf, F., Rieck, B., Niethammer, M., and Kwitt, R. Graph filtration learning. In Daumé III, H. and Singh, A. (eds.), *Proceedings of the 37th International Conference on Machine Learning (ICML)*, number 119 in Proceedings of Machine Learning Research, pp. 4314–4323. PMLR, 2020.
- Horn, M., De Brouwer, E., Moor, M., Moreau, Y., Rieck, B., and Borgwardt, K. Topological graph neural networks. In *International Conference on Learning Representations (ICLR)*, 2022. URL <https://openreview.net/forum?id=oxxUMeFwEHd>.
- Irwin, J. J. and Shoichet, B. K. ZINC—a free database of commercially available compounds for virtual screening. *J. Chem. Inf. Model.*, 45(1):177–182, January 2005.
- Jiang, W. and Luo, J. Graph neural network for traffic forecasting: A survey. *Expert Systems with Applications*, 207: 117921, nov 2022. doi: 10.1016/j.eswa.2022.117921.
- Jin, W., Barzilay, R., and Jaakkola, T. Junction tree variational autoencoder for molecular graph generation, 2018. URL <https://arxiv.org/abs/1802.04364>.
- Jin, W., Wohlwend, J., Barzilay, R., and Jaakkola, T. Iterative refinement graph neural network for antibody sequence-structure co-design, 2021. URL <https://arxiv.org/abs/2110.04624>.
- Jiradilok, P. and Kamtue, S. Transportation distance between probability measures on the infinite regular tree, 2021. URL <https://arxiv.org/abs/2107.09876>.
- Jost, J. and Liu, S. Ollivier’s ricci curvature, local clustering and curvature dimension inequalities on graphs. 2011. doi: 10.48550/ARXIV.1103.4037. URL <https://arxiv.org/abs/1103.4037>.
- Jumper, J., Evans, R., Pritzel, A., Green, T., Figurnov, M., Ronneberger, O., Tunyasuvunakool, K., Bates, R., Žídek, A., Potapenko, A., Bridgland, A., Meyer, C., Kohl, S. A. A., Ballard, A. J., Cowie, A., Romera-Paredes, B., Nikolov, S., Jain, R., Adler, J., Back, T., Petersen, S., Reiman, D., Clancy, E., Zielinski, M., Steinegger, M., Pacholska, M., Berghammer, T., Bodenstein, S., Silver, D., Vinyals, O., Senior, A. W., Kavukcuoglu, K., Kohli, P., and Hassabis, D. Highly accurate protein structure prediction with alphafold. *Nature*, 596(7873):583–589, Aug 2021. ISSN 1476-4687. doi: 10.1038/s41586-021-03819-2. URL <https://doi.org/10.1038/s41586-021-03819-2>.
- Justel, A., Peña, D., and Zamar, R. A multivariate kolmogorov-smirnov test of goodness of fit. *Statistics & Probability Letters*, 35(3):251–259, 1997. ISSN 0167-7152. doi: 10.1016/S0167-7152(97)00020-5.
- Kipf, T. N. and Welling, M. Semi-supervised classification with graph convolutional networks, 2016. URL <https://arxiv.org/abs/1609.02907>.
- Koolen, J. H., Markowsky, G., and Park, J. On electric resistances for distance-regular graphs. *European Journal of Combinatorics*, 34(4):770–786, 2013. ISSN 0195-6698. doi: 10.1016/j.ejc.2012.12.001.
- Li, M. L., Dong, M., Zhou, J., and Rush, A. M. A hierarchy of graph neural networks based on learnable local features, 2019. URL <https://arxiv.org/abs/1911.05256>.
- Li, P., Wang, Y., Wang, H., and Leskovec, J. Distance encoding: Design provably more powerful neural networks for graph representation learning, 2020. URL <https://arxiv.org/abs/2009.00142>.
- Liao, R., Li, Y., Song, Y., Wang, S., Nash, C., Hamilton, W. L., Duvenaud, D., Urtasun, R., and Zemel, R. S. Efficient graph generation with graph recurrent attention networks, 2019. URL <https://arxiv.org/abs/1910.00760>.
- Liu, S., Münch, F., and Peyerimhoff, N. Bakry–émery curvature and diameter bounds on graphs. *Calculus of Variations and Partial Differential Equations*, 57(2), mar 2018. doi: 10.1007/s00526-018-1334-x.
- Lovász, L. Random walks on graphs: A survey. In Miklós, D., Sós, V. T., and Szőnyi, T. (eds.), *Combinatorics, Paul Erdős is Eighty*, volume 2, pp. 353–398. János Bolyai Mathematical Society, Budapest, 1996.
- Mirhoseini, A., Goldie, A., Yazgan, M., Jiang, J. W., Songhori, E., Wang, S., Lee, Y.-J., Johnson, E., Pathak, O., Nazi, A., Pak, J., Tong, A., Srinivasa, K., Hang, W., Tuncer, E., Le, Q. V., Laudon, J., Ho, R., Carpenter, R., and Dean, J. A graph placement methodology for fast chip design. *Nature*, 594(7862):207–212, 2021. doi: 10.1038/s41586-021-03544-w.
- Monti, F., Frasca, F., Eynard, D., Mannion, D., and Bronstein, M. M. Fake news detection on social media using geometric deep learning, 2019. URL <https://arxiv.org/abs/1902.06673>.
- Moreno, S., Neville, J., and Kirshner, S. Tied kronecker product graph models to capture variance in network populations. *ACM Trans. Knowl. Discov. Data*, 12(3), 2018. ISSN 1556-4681. doi: 10.1145/3161885.
- Morris, C., Ritzert, M., Fey, M., Hamilton, W. L., Lenssen, J. E., Rattan, G., and Grohe, M. Weisfeiler and Leman go neural: Higher-order graph neural networks. *Proceedings of the AAAI Conference on Artificial Intelligence*, 33(1): 4602–4609, 2019. doi: 10.1609/aaai.v33i01.33014602.

- Morris, C., Kriege, N. M., Bause, F., Kersting, K., Mutzel, P., and Neumann, M. Tudataset: A collection of benchmark datasets for learning with graphs, 2020. URL <https://arxiv.org/abs/2007.08663>.
- Niu, C., Song, Y., Song, J., Zhao, S., Grover, A., and Ermon, S. Permutation invariant graph generation via score-based generative modeling, 2020. URL <https://arxiv.org/abs/2003.00638>.
- O’Bray, L., Horn, M., Rieck, B., and Borgwardt, K. Evaluation metrics for graph generative models: Problems, pitfalls, and practical solutions. In *International Conference on Learning Representations (ICLR)*, 2022.
- Ollivier, Y. Ricci curvature of metric spaces. *Comptes Rendus Mathématique*, 345(11):643–646, 2007. ISSN 1631-073X. doi: 10.1016/j.crma.2007.10.041.
- Papp, P. A. and Wattenhofer, R. A theoretical comparison of graph neural network extensions, 2022. URL <https://arxiv.org/abs/2201.12884>.
- Ruiz, C., Zitnik, M., and Leskovec, J. Identification of disease treatment mechanisms through the multiscale interactome. *Nat. Commun.*, 12(1):1796, March 2021.
- Sabanayagam, M., Vankadara, L. C., and Ghoshdastidar, D. Graphon based clustering and testing of networks: Algorithms and theory, 2021. URL <https://arxiv.org/abs/2110.02722>.
- Samal, A., Sreejith, R. P., Gu, J., Liu, S., Saucan, E., and Jost, J. Comparative analysis of two discretizations of ricci curvature for complex networks. *Scientific Reports*, 8(1), 2018. doi: 10.1038/s41598-018-27001-3.
- Saucan, E., Samal, A., and Jost, J. A simple differential geometry for complex networks, 2020. URL <https://arxiv.org/abs/2004.11112>.
- Togninalli, M., Ghisu, E., Llinares-López, F., Rieck, B., and Borgwardt, K. Wasserstein Weisfeiler–Lehman graph kernels, 2019. URL <https://arxiv.org/abs/1906.01277>.
- Topping, J., Di Giovanni, F., Chamberlain, B. P., Dong, X., and Bronstein, M. M. Understanding over-squashing and bottlenecks on graphs via curvature, 2021. URL <https://arxiv.org/abs/2111.14522>.
- van der Hoorn, P., Lippner, G., Trugenberger, C., and Krioukov, D. Ollivier curvature of random geometric graphs converges to ricci curvature of their riemannian manifolds, 2020. URL <https://arxiv.org/abs/2009.04306>.
- Vellingker, A., Sinop, A. K., Ktena, I., Veličković, P., and Gollapudi, S. Affinity-aware graph networks, 2022. URL <https://arxiv.org/abs/2206.11941>.
- Watts, D. J. and Strogatz, S. H. Collective dynamics of ‘small-world’ networks. *Nature*, 393(6684):440–442, 1998. doi: 10.1038/30918.
- Xu, K., Hu, W., Leskovec, J., and Jegelka, S. How powerful are graph neural networks? In *International Conference on Learning Representations*, 2019. URL <https://openreview.net/forum?id=ryGs6iA5Km>.
- You, J., Ying, R., Ren, X., Hamilton, W. L., and Leskovec, J. Graphrnn: Generating realistic graphs with deep auto-regressive models, 2018. URL <https://arxiv.org/abs/1802.08773>.

## A. Additional Proofs on Stability and Expressivity

### A.1. Stability Proofs

**Theorem 1.** *Given two graphs  $F = (V_F, E_F)$  and  $G = (V_G, E_G)$  with scalar-valued filtration functions  $f, g$ , and their respective persistence diagrams  $D_f, D_g$ , we have*

$$d_B(D_f, D_g) \leq \max\{\text{dis}(f, g), \text{dis}(g, f)\}, \quad (7)$$

where  $\text{dis}(f, g) := |\max_{x \in V_F} f(x) - \min_{y \in V_G} g(y)|$  and vice versa for  $\text{dis}(g, f)$ .

*Proof.* Considering the calculation of persistence diagrams based on scalar-valued filtrations functions, every point in the persistence diagram  $D_f$  can be written as a tuple of the form  $(f(v_F), f(v'_F))$ , with  $v_F, v'_F \in V_F$ ; the same applies for  $D_g$ . The inner distance between such tuples that occur in the bottleneck distance calculation can thus be written as

$$\|(f(v_F), f(v'_F)) - (g(v_G), g(v'_G))\|_\infty. \quad (14)$$

The maximum distance that can be achieved using this expression is determined by the maximum variation of the functions, expressed via  $\text{dis}(f, g)$  and  $\text{dis}(g, f)$ , respectively.  $\square$

**Graph perturbations.** Here we explicitly specify a common framework used in the proofs for stability of curvature functions. As mentioned in the main text, we consider perturbations to *unweighted, connected* graphs  $G = (V, E)$ , with  $|V| = n$  and  $|E| = m$ . In the case of *edge addition*, let  $i^*$  and  $j^*$  be arbitrary vertices that we wish to connect with a *new* edge, forming our new graph  $G' = (V, E')$  where  $E' = E \cup (i^*, j^*)$  such that  $|E'| = m + 1$ . For *edge deletion*, we similarly let  $(i^*, j^*) \in E$  be the edge we delete such that  $E' \subset E$  and  $|E'| = m - 1$ . Moreover, we only consider edges  $(i^*, j^*)$  that leave  $G'$  connected.

#### A.1.1. FORMAN–RICCI CURVATURE

**Theorem 2.** *If  $G'$  is the graph generated by **edge addition**, then the updated Forman curvature  $\kappa'_{FR}$  for pre-existing edges  $(i, j) \in E$  can be bounded by:*

$$\kappa_{FR}(i, j) - 1 \leq \kappa'_{FR}(i, j) \leq \kappa_{FR}(i, j) + 2. \quad (8)$$

*Proof.* By definition  $\kappa_{FR}(i, j)$  depends *only* on the degrees of the source and target  $(i, j) \in E$  and the number of triangles formed using  $(i, j)$ ,  $|\#\Delta_{ij}| = |N(i) \cup N(j)|$ , where  $N(i), N(j)$  are the set of neighbouring nodes for  $i, j$  respectively. This is a local computation— all relevant information can be computed in the subgraph generated by  $N(i) \cup N(j)$ . Thus, in order to understand stability of  $\kappa_{FR}$ , we need to understand how  $N(i)$  and  $N(j)$  change under graph perturbations. For our new graph  $G'$ , the only affected edges lie in the set:

$$E_{ij} := \{(u, v) \in E \mid u, v \in N(i) \cup N(j)\}$$

For the new edge  $(i^*, j^*)$ , we can directly compute  $\kappa_{FR}(i^*, j^*)$  based on the original structure of the graph. However, in terms of stability we are interested in the member of  $E_{ij}$ , which can be split into two cases: one of the nodes is  $i^*$  or  $j^*$  or neither is. *Case 1:* WLOG assume the edge is of the form  $(i^*, v) \in E_{ij}$ . Clearly,  $d'_i = d_i + 1$ . As for  $|\#\Delta_{iv}|$ , this can maximally be increased by 1 in the case that  $x \in S(i) \cap S(j)$ , else the triangle count stays the same. *Case 2:* consider  $(u, v) \in E_{ij}$  where  $u, v \in V \setminus \{i^*, j^*\}$ . In this case, there is no change to the degree nor the number  $|\#\Delta_{uv}|$ . Clearly then, if  $(i^*, j^*)$  forms a new triangle, our curvature can increase by 2, and if no triangle is formed the curvature can decrease by 1 in response to the increased degree. Thus we can bound  $\kappa'_{FR}(i, j) := 4 - d'_i - d'_j + 3|\#\Delta_{ij}|$  as follows:

$$\kappa_{FR}(i, j) - 1 \leq \kappa'_{FR}(i, j) \leq \kappa_{FR}(i, j) + 2$$

$\square$

**Theorem 3.** *If  $G'$  is the graph generated by **edge deletion**, then the updated Forman curvature  $\kappa'_{FR}$  for pre-existing edges  $(i, j) \in E$  can be bounded as follows:*

$$\kappa_{FR}(i, j) - 2 \leq \kappa'_{FR}(i, j) \leq \kappa_{FR}(i, j) + 1. \quad (9)$$

*Proof.* Again, we need only consider the edges in  $E_{ij}$ , as defined in the proof above, and can make the same case argument. *Case 1:* WLOG assume the edge is of the form  $(i^*, v) \in E_{ij}$ . Clearly,  $d'_i = d_i - 1$ . As for  $|\#\prime_{\Delta_{iv}}|$ , this can maximally be decreased by 1. *Case 2:* Degree and number of triangles do not change in response to the perturbation. Thus the following bounds hold for  $\kappa'_{\text{FR}}$ :

$$\kappa_{\text{FR}}(i, j) - 2 \leq \kappa'_{\text{FR}}(i, j) \leq \kappa_{\text{FR}}(i, j) + 1$$

□

### A.1.2. OLLIVIER–RICCI CURVATURE

The definition of  $\kappa_{\text{OR}}$  establishes a relationship between the graph metric  $d_G$ , the Wasserstein distance  $W_1$ , the probability distributions  $\mu_i, \mu_j$  at nodes  $i, j$  and the curvature. Given that we are considering unweighted, and connected graphs we know that  $(V, d_G)$  is a well-defined metric space and therefore  $W_1$  (as defined in Ollivier (2007)) defines the  $L_1$  transportation distance between two probability measures  $\mu_i, \mu_j$  with respect to the metric  $d_G$ . This is relevant for a much larger class of graph metrics than just the standard choice of the shortest path distance. We use results from Ollivier (2007) and the metric properties of  $W_1$  and  $d_G$  on graphs to bound the potential changes in  $\kappa_{\text{OR}}$  following an edge perturbation.

**Lemma 1.** *Consider the triple  $\mathcal{G} = (G, d_G, \mu)$ . Let  $\delta_i$  denote the Dirac measure at node  $i$  and  $J(i) := W_1(\delta_i, \mu_i)$  the corresponding jump probability in the graph  $G$ . The Ollivier–Ricci curvature  $\kappa_{\text{OR}}(i, j)$  satisfies the following Bonnet-Myers inspired upper bound:*

$$\kappa_{\text{OR}}(i, j) \leq \frac{J(i) + J(j)}{d_G(i, j)} \quad (15)$$

*Proof.* Rearranging the original definition for OR curvature gives:

$$W_1(\mu_i, \mu_j) = d_G(i, j)(1 - \kappa_{\text{OR}}(i, j))$$

By definition of the  $W_1$ , we have  $d_G(i, j) = W_1(\delta_i, \delta_j)$ . Using this and the fact that  $W_1$  satisfies the triangle inequality property, we can construct the desired upper bound on  $\kappa_{\text{OR}}$ :

$$\begin{aligned} d_G(i, j) &\leq W_1(\delta_i, \mu_i) + W_1(\mu_i, \mu_j) + W_1(\mu_j, \delta_j) \\ d_G(i, j) &\leq J(i) + d_G(i, j)(1 - \kappa_{\text{OR}}(i, j)) + J(j) \\ d_G(i, j)(1 - (1 - \kappa_{\text{OR}}(i, j))) &\leq J(i) + J(j) \\ \kappa_{\text{OR}}(i, j) &\leq \frac{J(i) + J(j)}{d_G(i, j)} \end{aligned}$$

□

**Theorem 4.** *Given a perturbation producing  $\mathcal{G}'$ ,  $\kappa'_{\text{OR}}$  can be bounded above using  $d_{G'}$  and jump probabilities  $J'(v) = W'_1(\delta_v, \mu'_v)$ :*

$$\kappa'_{\text{OR}} \leq \frac{J'(i) + J'(j)}{d_{G'}(i, j)}. \quad (10)$$

*Proof.* Given that  $G'$  is still connected, and both  $W'_1$  and  $d_{G'}$  still satisfy the metric axioms, this result follows directly from Lemma Lemma 1. □

**Theorem 5.** *Given a perturbation that yields  $\mathcal{G}' = (G, d_{G'}, \mu')$ ,  $\kappa'_{\text{OR}}$  can be bounded below by:*

$$\kappa'_{\text{OR}}(i, j) \geq 1 - \frac{1}{d_{G'}(i, j)} [2W'_{\max} + W'_1(\mu_i, \mu_j)]. \quad (11)$$

*Proof.* Recall from Section 3.1.2 that  $\mathcal{G}' = (G', d_{G'}, \mu')$  specifies the behaviour of the new graph metric  $d_{G'}$  and the updated probability measure  $\mu'$  in response to the perturbation. Moreover, this defines a new Wasserstein distance  $W'_1$  and we will show that the maximum reaction (as evaluated by  $W'_1$ ) to the perturbation  $W'_{\max} := \max_{x \in V} W'_1(\mu'_x, \mu_x)$  can

be used to express a general lower bound for OR curvature in the event of a perturbation. As per Eq. (4), we can define our curvature following the perturbation as:

$$\kappa'_{\text{OR}}(i, j) = 1 - \frac{1}{d_{G'}(i, j)} W'_1(\mu'_i, \mu'_j) \quad (16)$$

Once again, we can make use of the metric properties of  $W'_1$ , to establish a lower bound:

$$\begin{aligned} \kappa'_{\text{OR}}(i, j) &\geq 1 - \frac{1}{d_{G'}(i, j)} [W'_1(\mu_i, \mu'_i) + W'_1(\mu_j, \mu'_j) + W'_1(\mu_i, \mu_j)] \\ &\geq \frac{1}{d_{G'}(i, j)} [2W'_{\max} + W'_1(\mu_i, \mu_j)] \end{aligned}$$

□

### A.1.3. RESISTANCE CURVATURE

The resistance distance, intuitively, measures how well connected two nodes are in a graph. It is defined in Devriendt & Lambiotte (2022) as:

$$R_{ij} := (\mathbf{e}_i - \mathbf{e}_j)^\top Q^\dagger (\mathbf{e}_i - \mathbf{e}_j) \quad (17)$$

Here  $Q$  is the normalized laplacian (weighted degrees on the diagonal, see Devriendt & Lambiotte (2022)),  $Q^\dagger$  the Moore-Penrose inverse, and  $\mathbf{e}_i$  is  $i^{\text{th}}$  unit vector. This is the main feature that will be studied to understand the stability of the curvature measure, and can be computed for any two nodes in a connected component of a graph.

*A brief aside regarding the practice of inverting edge weights:* The common practice when computing effective resistance is to invert the edge weights of a graph in order to get a resistance. Given the spirit of resistance from circuit theory, we know that a high resistance should make it difficult for current to pass between nodes. Analogously when thinking about our graph as a markov chain, this would correspond to a low transition probability. So, if we think about our edge weights as coming from some kernel where higher similarity results in a higher edge weight, then we should definitely invert our edge weights to get to resistance. However, in the case that our edge weights represent the cost of travelling between nodes, then this is a suitable proxy for resistance in which case inverting the nodes is unnecessary. In order to achieve the theoretical properties of curvature with well known examples described in Devriendt & Lambiotte (2022), we *do not* invert the edge weights in our experiments. Which means that the curvature itself interprets the edge weights themselves as a cost/resistance; I think is an important point to specify especially given the similarity to markov chains and the borrowed terminology from circuit theory.

Recalling the equations for node resistance curvature 5, and resistance curvature 6, it becomes clear that the main task is to understand how the resistance distance changes in response to perturbations. The results below from Lovász (1996), are crucial for our proofs. Let  $C(i, j)$  be the commute time between nodes  $i, j \in V$ . It is important to note that these results depend on the *normalized Laplacian*, defined in Lovász (1996) as  $N = D^{\frac{1}{2}} A D^{\frac{1}{2}}$ , with eigenvalues  $\lambda_i$ , ordered such that  $\lambda_1 \geq \lambda_2 \geq \dots$ . Here,  $D$  is the diagonal matrix with inverse degrees and  $A$  the adjacency matrix. Also, as is consistent with the rest of the paper, assume our graph has  $n$  nodes and  $m$  edges, and  $d_i$  is the degree at node  $i \in V$ .

**Proposition 3.** *For a graph  $G$ , let  $N = D^{\frac{1}{2}} A D^{\frac{1}{2}}$  be the normalized Laplacian with eigen values  $\lambda_1 \geq \lambda_2 \geq \dots \geq \lambda_n$ . Then, the commute time in  $G$  between nodes  $i, j$  is subject to the following bounds:*

$$m \left( \frac{1}{d_s} + \frac{1}{d_t} \right) \leq C(i, j) \leq \frac{2m}{1 - \lambda_2} \left( \frac{1}{d_s} + \frac{1}{d_t} \right) \quad (18)$$

**Proposition 4.** *Consider the unweighted graph  $G$ , where each edge represents a unit resistance, i.e we consider each edge in the graph to be artificially weighted with value 1. Then the following equality holds for the commute time between nodes  $i, j$ :*

$$C(i, j) = 2m R_{ij} \quad (19)$$

**Proposition 5.** *If  $G'$  arises from a graph  $G$  by adding a new edge, then the commute time  $C'(i, j)$  between any two nodes in  $G'$  is bounded by:*

$$C'(i, j) \leq \left(1 + \frac{1}{m}\right)C(i, j) \quad (20)$$

For proofs of these propositions, we refer the reader to Lovász (1996). These results create a direct connection between commute times and resistance distance, and gives insight into how commute time reacts under edge addition, and we use them directly to generate our bounds for resistance curvature.

**Theorem 6.** *If  $G'$  is the graph generated by **edge addition**, then  $\kappa'_R \geq \kappa_R$ , with the following bound:*

$$|\kappa'_R(i, j) - \kappa_R(i, j)| \leq \frac{\Delta_{add}(d_i + d_j)}{R_{ij} - \Delta_{add}}, \quad (12)$$

where  $\Delta_{add} := \max_{i, j \in V} \left(R_{ij} - \frac{1}{2} \left(\frac{1}{d_i+1} + \frac{1}{d_j+1}\right)\right)$ .

*Proof.* Let  $R'_{ij}$  be the resistance distance in  $G'$ . Likewise, let  $C(i, j)$  be the commute distance in  $G$  between nodes  $i, j$  and  $C'(i, j)$  be the commute time in  $G'$ . Then 20 and 19 ensure that  $R'_{ij}$  is bounded above, by the original resistance distance in  $G$ :

$$\begin{aligned} 2(m+1)R'_{ij} &\leq 2m\left(1 + \frac{1}{m}\right)R_{ij} \\ R'_{ij} &\leq R_{ij} \end{aligned}$$

This follows our intuition of resistance distance very well: with the addition of an edge nodes can only get more connected. 18 also gives a nice lower bound:

$$\begin{aligned} (m+1)\left(\frac{1}{d'_i} + \frac{1}{d'_j}\right) &\leq C'(i, j) \\ \frac{1}{2}\left(\frac{1}{d'_i} + \frac{1}{d'_j}\right) &\leq R'_{ij} \end{aligned}$$

In the case that we are adding a single edge, it is often the case that  $d'_x = d_x$ . However, the nodes that are connected by the new edge,  $(i^*, j^*) \in E' \setminus E$ , increase such that  $d'_{i^*} = d_{i^*} + 1$  and  $d'_{j^*} = d_{j^*} + 1$ . Thus, the following lower bound holds in general for  $R'_{ij}$  and we can remain agnostic to the precise location of the new edge:

$$\frac{1}{2}\left(\frac{1}{d_i+1} + \frac{1}{d_j+1}\right) \leq R'_{ij} \leq R_{ij} \quad (21)$$

And likewise, after adding  $p$  edges:

$$\frac{1}{2}\left(\frac{1}{d_i+p} + \frac{1}{d_j+p}\right) \leq R^p_{ij} \leq R_{ij}$$

So the bounds of our 'perturbed' resistance distance  $R'_{ij}$  are determined by the initial network structure ( $R_{ij}$ ) and the number connections each specific vertex has. Naturally, certain node pairs will be more strongly affected by the addition of an edge. We can define the maximum reaction to perturbation across pairs as follows:

$$\Delta_{add} := \max_{i, j \in V} \left(R_{ij} - \frac{1}{2}\left(\frac{1}{d_i+1} + \frac{1}{d_j+1}\right)\right) \quad (22)$$

This can be used to bound node resistance curvature. In an unweighted graph, we have

$$p_i = 1 - \frac{1}{2} \sum_{j \sim i} R_{ij}$$

$$p'_i = 1 - \frac{1}{2} \sum_{j \sim i} R'_{ij}$$

For  $G$  and  $G'$  respectively. Given that resistance can only increase,  $p_i$  is clearly an lower bound for  $p'_i$ . Certainly a lower bound occurs when when the resistance between each one of  $i$ 's neighbors maximally decreases. Thus we get the following inequality:

$$p_i \leq p'_i \leq p_i + \frac{d_i}{2} \Delta_{add}$$

Finally this gives the desired bound on  $\kappa'_R$ :

$$\kappa_R(i, j) \leq \kappa'_R(i, j) \leq \kappa_R(i, j) + \frac{\Delta_{add}(d_i + d_j)}{R_{ij} - \Delta_{add}}$$

□

**Theorem 7.** *If  $G'$  is the graph generated by **edge deletion**, then  $\kappa'_R \leq \kappa_R$ , bounded by:*

$$|\kappa'_R(i, j) - \kappa_R(i, j)| \leq \frac{1}{R_{ij} + \Delta_{del}} \left[ \frac{2}{R_{ij}} (2R_{ij} + \Delta_{del})(p_i + p_j) - \Delta_{del}(d_i + d_j) \right],$$

where  $\Delta_{del} = \frac{2}{1 - \lambda_2} - \min_{i, j \in V} (R_{ij})$  and  $\lambda_2$  is the second largest eigenvalue of  $N$ .

*Proof.* Now we can beg the question of how effective resistance changes when we remove an edge. By inverting our initial argument in above proof of 6, we know that after removing an edge our resistance distance can only increase. Formally,  $R_{ij} \leq R'_{ij}$ . For the upper bound, we can once again make an argument using 18, this time relying on the other half of the inequality. Here we need to also mention the normalized Laplacian  $N'$  for  $G'$ , with eigenvalues  $\lambda'_1 \geq \lambda'_2 \geq \dots \geq \lambda'_n$ .

$$C'(i, j) \leq \frac{2(m-1)}{1 - \lambda'_2} \left( \frac{1}{d'_i} + \frac{1}{d'_j} \right)$$

$$R'_{ij} \leq \frac{1}{1 - \lambda'_2} \left( \frac{1}{d'_i} + \frac{1}{d'_j} \right)$$

Again, we know that only the two unique vertices  $(i^*, j^*)$  that shared an edge will have affected degrees, s.t  $d'_{i^*} = d_{i^*} - 1$  and  $d'_{j^*} = d_{j^*} - 1$ . Moreover, from Guo et al. (2018), we know that  $\lambda_2 \geq \lambda'_2$ . So we can bound the  $R'_{ij}$  as follows:

$$R_{ij} \leq R'_{ij} \leq \frac{2}{1 - \lambda_2} \quad (23)$$

In fact, this applies to any number of edge deletions, as long as  $G'$  stays connected. Again, we can define a maximum possible change in resistance distance across the graph:

$$\Delta_{del} = \max_{i, j \in V} \left( \frac{2}{1 - \lambda_2} - R_{ij} \right) = \frac{2}{1 - \lambda_2} - \min_{i, j \in V} (R_{ij}) \quad (24)$$

This leads to the following bounds on node and edge curvature, and completes the proof:

$$p_i - \frac{d_i}{2} \Delta_{del} \leq p'_i \leq p_i$$

$$(1 - \lambda_2) \left[ p_i + p_j - \frac{\Delta_{del}}{2} (d_i + d_j) \right] \leq \kappa'_R(i, j) \leq \kappa_R(i, j)$$

$$\kappa_R(i, j) - \frac{1}{R_{ij} + \Delta_{del}} \left[ \frac{2}{R_{ij}} (2R_{ij} + \Delta_{del})(p_i + p_j) - \Delta_{del}(d_i + d_j) \right] \leq \kappa'_R(i, j) \leq \kappa_R(i, j)$$

□



## A.2. Expressivity Proofs

**Theorem 8.** *Given two graphs  $F = (V_F, E_F)$  and  $G = (V_G, E_G)$  with scalar-valued filtration functions  $f, g$ , and their respective persistence diagrams  $D_f, D_g$ , we have*

$$d_B(D_f, D_g) \geq \inf_{\eta: V_F \rightarrow V_G} \sup_{x \in V_F} |f(x) - g(\eta(x))|, \quad (13)$$

where  $\eta$  ranges over all maps from  $V_F$  to  $V_G$ .

*Proof.* Considering the calculation of persistence diagrams based on scalar-valued filtrations functions, every point in the persistence diagram  $D_f$  can be written as a tuple of the form  $(f(v_F), f(v'_F))$ , with  $v_F, v'_F \in V_F$ ; the same applies for  $D_g$ . The inner distance between such tuples that occur in the bottleneck distance calculation can thus be written as

$$\|(f(v_F), f(v'_F)) - (g(v_G), g(v'_G))\|_\infty, \quad (25)$$

which we can rewrite to  $\max_{C: V_F \rightarrow V_G} \{f(x) - g(C(x))\}$  for a general map  $C$  induced by the bijection of the bottleneck distance. Not every map is induced by a bijection, though. Hence, if we maximise over *arbitrary* maps between the vertex sets, we are guaranteed to never exceed the bottleneck distance.  $\square$

## B. Additional Proofs for Distinguishing Strongly Regular Graphs

**Proposition 1.** *Both Forman–Ricci curvature and Resistance curvature cannot distinguish distance-regular graphs with the same intersection array.*

*Proof.* We first show the part of the statement relating to the *Forman–Ricci curvature*. Given a distance-regular graph  $G$  with  $N$  vertices and intersection array  $\{b_0, b_1, \dots, b_{D-1}; c_1, c_2, \dots, c_D\}$ . Let  $i, j$  be adjacent nodes in  $G$ . For a regular graph, we have  $d_i = d_j = b_0$ , where  $b_0$  is a constant. The number of triangles between two adjacent nodes  $i$  and  $j$  in  $G$  is given by  $a_1 = b_0 - b_1 - c_1$  (Dam et al., 2016). The Forman curvature of  $i, j$  is thus

$$\kappa_{\text{FR}}(i, j) := 4 - 2b_0 + 3|b_0 - b_1 - c_1|. \quad (26)$$

Given two strongly-regular graphs with the same intersection array, i.e. the same values of  $b_0, b_1$  and  $c_1$ , the Forman curvature yields the same value for all pairs of adjacent nodes and cannot distinguish them. For the *resistance curvature*, the claim follows as an immediate Corollary of Theorem A (Biggs, 1993) and described in Koolen et al. (2013). Given the resistance between two nodes depends only on the intersection array and the number of nodes in the graph, then the resistance curvature cannot distinguish two strongly-regular graphs.  $\square$

**Proposition 2.** *Ollivier–Ricci curvature can distinguish the Rook and Shrikhande graphs, which are strongly-regular graphs with the same intersection array.*

*Proof.* Both graphs have the same intersection array  $\{6, 3; 1, 2\}$  but differ in their first hop peripheral subgraphs (Feng et al., 2022). It is known that 2-WL cannot distinguish these graphs. Ollivier–Ricci curvature, however, is sensitive to these differences in peripheral subgraphs with the edge curvatures for the Rook graph being:  $[0.2, 0.2, 0.33, 0.33, 0.33, 0.2, 0.33, 0.33, 0.33, 0.33, 0.33, 0.33, 0.33, 0.33, 0.2, 0.2, 0.33, 0.33, 0.33, 0.33, 0.33, 0.33, 0.33, 0.33, 0.33, 0.33, 0.33, 0.2, 0.33, 0.33, 0.33, 0.33, 0.33, 0.33, 0.33, 0.33, 0.33, 0.33, 0.33, 0.33, 0.33, 0.33, 0.33, 0.33, 0.33]$ , and for the Shrikhande graph they are  $[0, 0, 0.27, 0.27, 0.1, 0, 0.27, 0.27, 0.1, 0, 0.27, 0.1, 0.27, 0, 0.27, 0.1, 0.27, 0, 0.1, 0.27, 0.27, 0.1, 0.27, 0.17]$ , demonstrating that OR curvature can distinguish these graphs—*unlike Resistance curvature, Forman–Ricci curvature and the 2-WL test.*  $\square$

## C. Additional Stability Analysis

Given the bounds on curvature established in Section 3.1.2, we explore how curvature changes experimentally by analysing edge perturbations on Erdős–Rényi graphs. In particular, we provide statistics that quantify the maximal change in curvature for random graphs with varying connectivity parameters in response to edge additions and deletions. The experiment fixes

the number of nodes in the ER graphs ( $n = 100$ ), and generates a sample of 50 graphs for the selected values of  $p$ . For each graph in the sample, we measure the curvature  $\kappa$  of all edges and calculate the standard deviation  $\sigma_\kappa$  of this distribution. We then perturb the original graph by edge addition/deletion and calculate the new curvature  $\kappa'$ . The following tables present the *worst case* deviations in curvature, which we define as  $\Delta\kappa = |\kappa - \kappa'|$ , in units of  $\sigma_\kappa$ ; in other words the maximal value of  $\Delta\kappa/\sigma_\kappa$  over all sample graphs and their edges.

Curvature	Edge Addition: Maximal Change ( $\downarrow$ ) in Curvature for ER Graphs ( $\Delta\kappa/\sigma_\kappa$ )									
	$p=0.1$	$p=0.2$	$p=0.3$	$p=0.4$	$p=0.5$	$p=0.6$	$p=0.7$	$p=0.8$	$p=0.9$	
$\kappa_{FR}$	0.582	0.419	0.334	0.296	0.253	0.246	0.232	0.25	0.315	
$\kappa_{OR}$	1.545	1.157	0.613	0.465	0.396	0.366	0.368	0.399	0.512	
$\kappa_R$	0.689	0.417	0.296	0.251	0.221	0.232	0.227	0.243	0.321	

Curvature	Edge Deletion: Maximal Change ( $\downarrow$ ) in Curvature for ER Graphs ( $\Delta\kappa/\sigma_\kappa$ )									
	$p=0.1$	$p=0.2$	$p=0.3$	$p=0.4$	$p=0.5$	$p=0.6$	$p=0.7$	$p=0.8$	$p=0.9$	
$\kappa_{FR}$	0.609	0.408	0.334	0.291	0.255	0.239	0.245	0.243	0.319	
$\kappa_{OR}$	1.397	1.27	0.623	0.479	0.394	0.365	0.347	0.402	0.482	
$\kappa_R$	0.75	0.431	0.336	0.248	0.229	0.218	0.225	0.242	0.312	

## D. Probability Measure for Ollivier–Ricci Curvature and Counting Substructures

The Ollivier–Ricci curvature is of particular interest because of its flexibility. While the predominant probability measure  $\mu$  used by the community is *uniform* for each node, i.e. each of the node’s neighbours is chosen with probability being proportional to the degree of the node. We experimented with different probability measures, one being based on expanding  $\mu$  to the two-hop neighbourhood of a vertex, the other one being based on random walk probabilities. Specifically, for a node  $x$  and a positive integer  $m$ , we calculate  $\mu_{RW}$  as

$$\mu_{RW}(y) := \sum_{k \leq m} \phi_k(x, y), \quad (27)$$

with  $\phi_k(x, y)$  denoting the probability of reaching node  $y$  in a  $k$ -step random walk that starts from node  $x$ . Subsequently, we normalise Eq. (27) to ensure that it is a valid probability distribution. In our experiments, we set  $m = 2$ , meaning that at most 2-step random walks will be considered. As shown in the main paper, this formulation leads to an increase in expressivity, and we expect that further exploration of the probability measures will be a fruitful direction for the future.

We now explore to what extent the ability of the curvature to count substructures can also be improved in this way. To do this, we used powers of the transition matrix as the probability measure, as it has been shown that the  $n$ th power provides information on the number of  $n$ -paths and can therefore provide substructure information for cycles of size  $n$  (Li et al., 2020). We find that powers of the transition matrix larger than 1 can perform better for counting the substructures, particularly for substructures larger than 3-cycles. There is also a difference between Regular and Erdős–Rényi (ER) graphs as the best transition power tends to be higher for ER graphs. We hypothesise that this may have something to do with the mixing time of the graph, as large powers should converge to the stationary distribution, and regular graphs are more ‘expander-like’. The best results are obtained by taking multiple landscapes using the transition matrix powers (up to  $n = 5$ ) and then averaging them. We show that combined with a single layer MLP, this method can perform better than using Graph Neural Network based approaches and OR curvature with the uniform measure.

Method	Counting Substructures (MAE $\downarrow$ )			
	Triangle	Tailed Tri.	Star	4-Cycle
GCN	0.4186	0.3248	<b>0.1798</b>	0.2822
$\kappa_{OR}$ Filtration	0.2321	0.2395	0.3393	0.3089
$\kappa_{OR}$ Filtration with transition matrix powers	<b>0.1956</b>	<b>0.2095</b>	0.3212	<b>0.2680</b>

## E. Computational Complexity

Persistence diagrams of 1-dimensional simplicial complexes, i.e. graphs, can be computed in  $\mathcal{O}(m \log m)$  time where  $m$  denotes the number of edges. Empirically, when calculating different curvature measures for different sizes of graphs, we

Method	Optimal Transition Power	
	ER	Regular
Triangle	2	1
Tailed Triangle	4	3
Star	4	2
Chordal Cycle	2	2
4-Cycle	8	3

Table 4: Computation time in seconds for discrete curvature on varying Erdős–Rényi graph sizes with  $p = 0.3$ .

No. nodes	$\kappa_{FR}$	$\kappa_{OR}$	$\kappa_R$
10	0.000	0.002	0.020
50	0.001	0.038	0.700
100	0.005	0.247	6.610
250	0.054	4.720	252.850
500	0.380	59.270	6414.970
1000	2.920	1040.700	74366.070

find that Forman curvature scales well to large graphs, whereas OR and resistance curvatures can be used for smaller graphs and in cases that require a more expressive measure. Note that there are significantly faster ways to calculate resistance curvature as an approximation Velingker et al. (2022). A majority of works on GGMs focus on small molecule generation, where any of these curvatures can be used with minimal pre-computation. Table 4 depicts the computational complexity of various curvature calculations on Erdős–Rényi graphs.

## F. Ethical Concerns

We have proposed a general framework for comparing graph distributions focusing primarily on method and theoretical development rather than on potential applications. We currently view drug discovery as being one of the main application areas, where further experiments may be required, but we have no evidence that our method enhances biases or causes harm in any way.